

Clouds and the atmospheric circulation response to warming

Article

Published Version

Ceppi, P. and Hartmann, D. L. (2016) Clouds and the atmospheric circulation response to warming. *Journal of Climate*, 29 (2). pp. 783-799. ISSN 1520-0442 doi: 10.1175/JCLI-D-15-0394.1 Available at <https://centaur.reading.ac.uk/46906/>

It is advisable to refer to the publisher's version if you intend to cite from the work. See [Guidance on citing](#).

To link to this article DOI: <http://dx.doi.org/10.1175/JCLI-D-15-0394.1>

Publisher: American Meteorological Society

All outputs in CentAUR are protected by Intellectual Property Rights law, including copyright law. Copyright and IPR is retained by the creators or other copyright holders. Terms and conditions for use of this material are defined in the [End User Agreement](#).

www.reading.ac.uk/centaur

CentAUR

Central Archive at the University of Reading

Clouds and the Atmospheric Circulation Response to Warming

PAULO CEPPI AND DENNIS L. HARTMANN

Department of Atmospheric Sciences, University of Washington, Seattle, Washington

(Manuscript received 2 June 2015, in final form 15 October 2015)

ABSTRACT

The authors study the effect of clouds on the atmospheric circulation response to CO_2 quadrupling in an aquaplanet model with a slab ocean lower boundary. The cloud effect is isolated by locking the clouds to either the control or 4xCO_2 state in the shortwave (SW) or longwave (LW) radiation schemes. In the model, cloud radiative changes explain more than half of the total poleward expansion of the Hadley cells, mid-latitude jets, and storm tracks under CO_2 quadrupling, even though they cause only one-fourth of the total global-mean surface warming. The effect of clouds on circulation results mainly from the SW cloud radiative changes, which strongly enhance the equator-to-pole temperature gradient at all levels in the troposphere, favoring stronger and poleward-shifted midlatitude eddies. By contrast, quadrupling CO_2 while holding the clouds fixed causes strong polar amplification and weakened midlatitude baroclinicity at lower levels, yielding only a small poleward expansion of the circulation. The results show that 1) the atmospheric circulation responds sensitively to cloud-driven changes in meridional and vertical temperature distribution and 2) the spatial structure of cloud feedbacks likely plays a dominant role in the circulation response to greenhouse gas forcing. While the magnitude and spatial structure of the cloud feedback are expected to be highly model dependent, an analysis of 4xCO_2 simulations of CMIP5 models shows that the SW cloud feedback likely forces a poleward expansion of the tropospheric circulation in most climate models.

1. Introduction

Clouds exert a very substantial effect on the energy balance of the earth's atmosphere through their effects on shortwave (SW) and longwave (LW) radiation, with an approximate global-mean effect of -20 W m^{-2} (Boucher et al. 2013). With increasing greenhouse gas forcing, the SW and LW radiative effects of clouds are expected to change, and while the magnitude of this change is highly uncertain, most climate models predict a positive global-mean forcing from cloud changes—a positive cloud feedback (Soden et al. 2008; Vial et al. 2013). Previous research has mainly focused on the impact of cloud feedbacks on the global energy balance and climate sensitivity (e.g., Soden et al. 2008; Zelinka and Hartmann 2010; Zelinka et al. 2012; Vial et al. 2013). However, cloud feedbacks also possess rich spatial structures, and hence, they affect spatial patterns of warming (Roe et al. 2015), meridional energy

transport by atmospheric motions (Hwang and Frierson 2010; Zelinka and Hartmann 2012), and likely also the atmospheric circulation (Ceppi et al. 2014; Voigt and Shaw 2015).

While quantitative aspects of the circulation response to greenhouse gas forcing remain highly uncertain, robust qualitative aspects of the response include a weakening of the Hadley circulation (Held and Soden 2006; Vecchi and Soden 2007), a rise of the tropopause and upward expansion of the circulation (e.g., Lorenz and DeWeaver 2007), and a poleward expansion of the Hadley cells, midlatitude jets, and storm tracks (Kushner et al. 2001; Yin 2005; Lu et al. 2007; Frierson et al. 2007; Chang et al. 2012; Barnes and Polvani 2013). How clouds contribute to shaping such circulation changes is presently not well understood. It is also unclear to what extent the uncertainty in the cloud feedbacks affects the intermodel spread in atmospheric circulation changes; it has been suggested that this effect

Corresponding author address: Paulo Ceppi, Department of Atmospheric Sciences, University of Washington, Box 351640, Seattle, WA 98195.
E-mail: ceppi@atmos.washington.edu

Publisher's Note: This article was revised on 29 January 2016 to correct a typographical error in Table 1.

could be substantial in the case of the midlatitude jet response (Ceppi et al. 2014).

The purpose of this paper is to quantitatively assess the effect of cloud radiative changes on the atmospheric circulation response to CO₂ increase in a climate model. Here, we use an aquaplanet model with interactive sea surface temperature to demonstrate that clouds can cause a very substantial enhancement of the circulation response to CO₂ quadrupling. Overall, clouds explain more than half of the total poleward expansion of the circulation in our model. This occurs mainly through the SW effect of clouds, which acts to strongly increase the equator-to-pole temperature gradient and make the midlatitudes more baroclinically unstable. Remarkably, CO₂ quadrupling only yields a weak poleward expansion of the circulation if the clouds are held fixed, indicating that the cloud response is a key influence on the circulation changes predicted by our model. Because clouds have such a strong effect, the results presented here suggest that cloud feedbacks could significantly contribute to the uncertainty in the atmospheric circulation response to global warming, highlighting the need for better constraints on the cloud response in climate models.

We begin by presenting the methodology used to isolate the effect of cloud radiative changes on atmospheric circulation in our climate model in section 2. In section 3, we then present the key results of our experiments, followed by a discussion in section 4, and a summary and concluding remarks in section 5.

2. Methods

The atmospheric model used in this study is the Geophysical Fluid Dynamics Laboratory Atmospheric Model, version 2.1 (GFDL AM2.1; [GFDL Global Atmospheric Model Development Team 2004](#)). It is run in aquaplanet configuration, coupled to a slab ocean lower boundary representing a mixed layer of 50 m depth. While there is no seasonal cycle, insolation is set to its annual-mean value at every latitude. The model also has no sea ice, but the sea surface temperature can be below freezing. We study the effects of cloud feedbacks on atmospheric circulation by comparing two model climatologies with identical boundary conditions except for CO₂ forcing. These two climates, which we describe as CTL and 4xCO₂, have CO₂ mixing ratios of 348 and 1392 ppm, respectively.

We use the cloud-locking method to assess the effect of cloud radiative changes on the atmospheric circulation response. This method involves prescribing clouds from two different climate states in the climate model's radiation code to obtain the effect of cloud changes in isolation. In our case, the two climate states that the clouds are "locked" to are CTL and 4xCO₂. Note that only the radiation code experiences the locked clouds, which override the cloud

radiative properties simulated by the model interactively; all other model components (e.g., the cloud microphysics or the large-scale condensation scheme) use the model's internally simulated clouds. Locking of model fields such as clouds and water vapor as a method to quantify feedback processes has been successfully implemented in many studies (e.g., Wetherald and Manabe 1980, 1988; Hall and Manabe 1999; Schneider et al. 1999; Langen et al. 2012; Mauritsen et al. 2013; Voigt and Shaw 2015). Unlike previous studies, however, we discriminate between SW and LW cloud effects by separately prescribing cloud radiative properties in the SW and LW radiation schemes.

When locking clouds, it is necessary to use the full time-varying cloud radiative properties, rather than time-averaged values. This is because cloud radiative properties (e.g., cloud optical depth) and cloud radiative effects are generally not linearly related, so that using time-mean cloud properties would yield a large climate bias. We therefore prescribe instantaneous cloud radiative properties taken from every call of the radiation code. As discussed in previous studies (Schneider et al. 1999; Mauritsen et al. 2013; Voigt and Shaw 2015), prescribing cloud properties at every time step results in the loss of the spatiotemporal correlation between cloud, moisture, and temperature anomalies, which may cause a bias in the mean climate. For example, the radiation code could experience cloud-free conditions in a grid box in which ascent and condensation are occurring, because the prescribed cloud radiative properties are decorrelated from the weather. We will show in the next section that this climate bias is small, however, and is unlikely to affect our conclusions. To ensure that variables are similarly decorrelated in all experiments, the prescribed cloud fields are offset by 1 year relative to the model's simulated climate.

The cloud-locked experiments are performed as follows. We first run the CTL and 4xCO₂ experiments with interactive clouds for 20 years (after discarding 2 years of model spinup) and save all cloud variables used in the model's radiation scheme at every call of the radiation code (every 6 h). We then use the cloud radiative properties output by the interactive CTL and 4xCO₂ simulations to run a total of eight cloud-locked simulations, involving all possible combinations of CO₂ concentration G, SW cloud radiative properties S, and LW cloud radiative properties L. Denoting the CTL and 4xCO₂ states by numbers 1 and 2, respectively, the eight experiments are G1S1L1, G2S1L2, G1S2L1, G1S1L2, G2S2L1, G2S1L2, G1S2L2, and G2S2L2. In each of these cloud-locked simulations, the time-varying cloud properties from either the CTL or 4xCO₂ simulation are read in at every time step and override the cloud properties calculated by the model. Separately locking SW and LW cloud radiative properties is possible because the AM2.1 radiation scheme uses different cloud properties in the SW and LW schemes.

Locking the model clouds allows us to calculate the separate effects of changing clouds while keeping CO₂ levels fixed, and increasing CO₂ while keeping the clouds fixed. For simplicity, hereafter we refer to these components as the “effect of cloud radiative changes,” and the “effect of CO₂ increase,” but it must be kept in mind that each of these effects includes additional contributions from other climate feedbacks (see discussion below). We calculate the effects of clouds and CO₂ increase using a method similar to Voigt and Shaw (2015) and follow their notation in the discussion below. Consider a variable X , which is a function of G, S, and L. The total response of X to changes in all of these variables can be written as

$$\delta X = X_{G2S2L2} - X_{G1S1L1}, \quad (1)$$

where the subscripts 1 and 2 refer to the control and perturbed states, respectively. The individual contributions of greenhouse gas forcing and cloud SW and LW effects can then be expressed as

$$\delta X_G = \frac{1}{2}[(X_{G2S1L1} - X_{G1S1L1}) + (X_{G2S2L2} - X_{G1S2L2})], \quad (2)$$

$$\begin{aligned} \delta X_S = & \frac{1}{4}[(X_{G1S2L1} - X_{G1S1L1}) + (X_{G2S2L1} - X_{G2S1L1}) \\ & + (X_{G1S2L2} - X_{G1S1L2}) + (X_{G2S2L2} - X_{G2S1L2})], \end{aligned} \quad (3)$$

$$\begin{aligned} \delta X_L = & \frac{1}{4}[(X_{G1S1L2} - X_{G1S1L1}) + (X_{G2S1L2} - X_{G2S1L1}) \\ & + (X_{G1S2L2} - X_{G1S2L1}) + (X_{G2S2L2} - X_{G2S2L1})], \end{aligned} \quad (4)$$

Equations (2)–(4) represent averages over the various pairs of experiments that involve changes in each of the three variables of interest. It can easily be shown that the right-hand sides of Eqs. (2)–(4) add up to the right-hand side of Eq. (1), so that $\delta X = \delta X_G + \delta X_S + \delta X_L$ by construction. In the remainder of this paper, for additional clarity, the terms δX_G , δX_S , and δX_L are referred to as δX_{CO_2} , $\delta X_{SW\ cloud}$, and $\delta X_{LW\ cloud}$, respectively. We additionally define the change in X due to the net cloud radiative change as the sum of the SW and LW effects, $\delta X_{net\ cloud} = \delta X_{SW\ cloud} + \delta X_{LW\ cloud}$.

It is important to note that the cloud and CO₂ responses in our experiments are affected by other feedbacks. In our model, this includes the temperature feedbacks (Planck and lapse rate), as well as the water vapor feedback; surface albedo values are kept constant between experiments. Unlike other studies (Langen et al. 2012; Mauritzen et al. 2013; Voigt and

Shaw 2015), we do not separately account for the positive water vapor feedback, which likely amplifies the anomalies caused by the CO₂ and cloud perturbations in our experiments. Thus, the “effect of cloud radiative changes” as defined in this paper encompasses all effects of replacing the clouds from the CTL climate with 4xCO₂ clouds, including subsequent temperature and water vapor feedbacks. The same applies to the component of the response that we ascribe to the CO₂ increase. This should be kept in mind in the interpretation of our results, since the water vapor feedback in isolation has been shown to have a nonnegligible effect on the atmospheric circulation response (Voigt and Shaw 2015).

3. Results

a. Climate response to CO₂ and cloud changes

We begin by describing the total response to CO₂ quadrupling, including the effects of cloud feedbacks, in the experiment with locked clouds (left column of Fig. 1); this is equivalent to the change described by Eq. (1). CO₂ quadrupling produces a large increase in sea surface temperature (SST), with a global-mean increase of 4.4 K and amplified warming at high latitudes (Fig. 1a, left). The surface warming is smallest near the edge of the tropics, so that the meridional SST gradient increases within the tropics but decreases in the extratropics. The vertical structure of the temperature response (Fig. 1b) features the familiar maximum in the upper tropical troposphere (as expected if the tropical troposphere remains close to neutral stability relative to the moist adiabat) and stratospheric cooling, a direct consequence of the CO₂ increase. The temperature changes result in a large zonal wind response (Fig. 1c) with a poleward shift of the tropospheric jet and a vertical expansion of the upper-level westerlies. The upper tropical troposphere also features a transition from easterly to superrotating winds at the equator, a feature previously reported in warmed aquaplanet climates (Caballero and Huber 2010), with westerly winds peaking near 8 m s⁻¹ around 100 hPa. Finally, the response of the mean meridional circulation reflects the combined effects of a Hadley cell weakening, and upward and poleward expansion of the circulation, all of which are typical features of global warming experiments (e.g., Frierson et al. 2006; Lorenz and DeWeaver 2007; Langen et al. 2012). Differences between hemispheres appear to be minimal, suggesting that the responses are very robust and unaffected by sampling variability.

Before we study the individual effects of cloud feedbacks and CO₂ increase on the circulation response, we

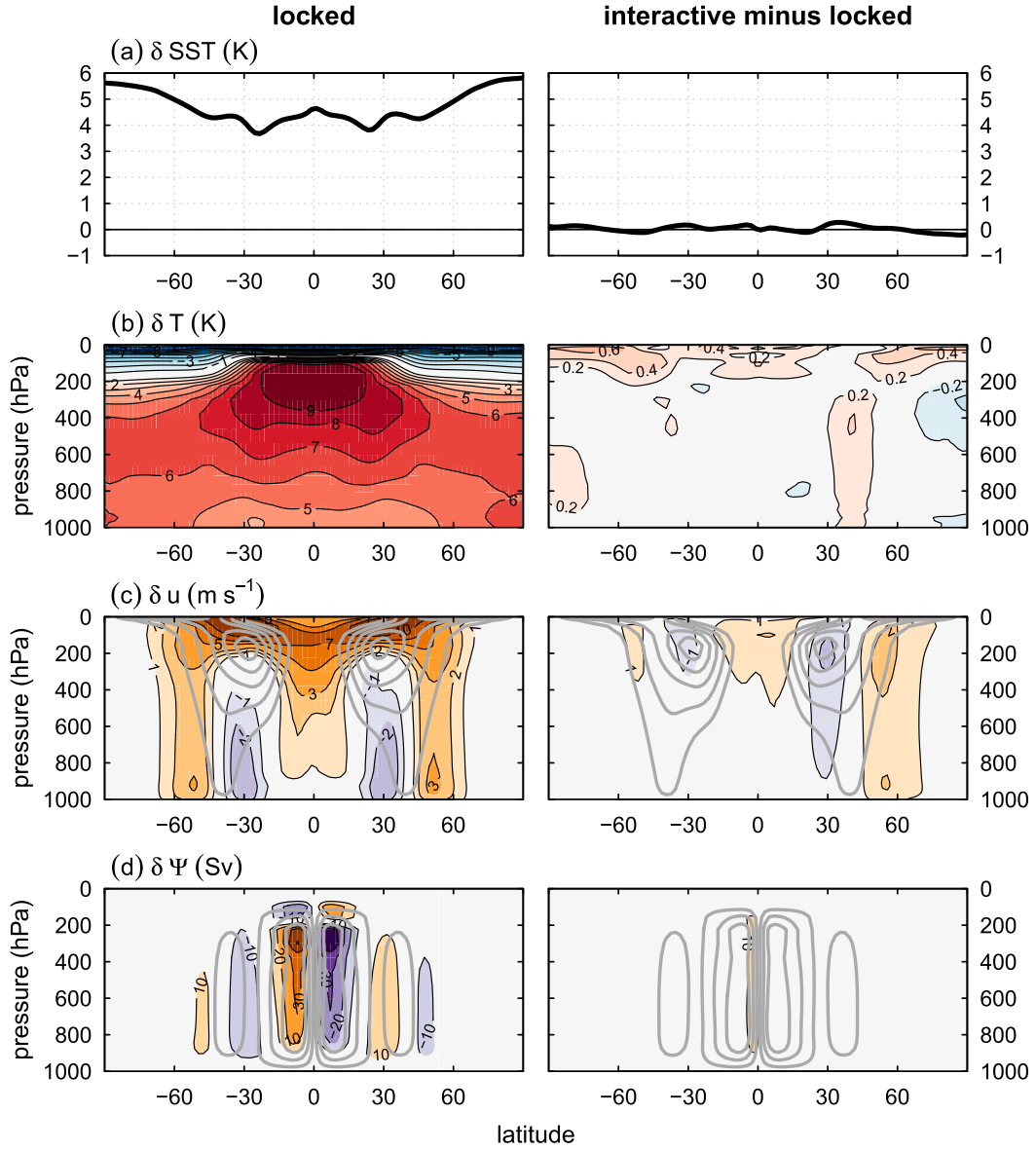


FIG. 1. Changes in (a) SST, (b) air temperature, (c) zonal wind, and (d) meridional mass streamfunction after CO_2 quadrupling. The left column shows the changes between the CTL and 4xCO_2 experiments, with clouds locked to CTL and 4xCO_2 climates, respectively [Eq. (1)]. The right column shows the difference between the response in cases with interactive and locked clouds. In (d), 1 Sv (mass based) = 10^9 kg s^{-1} .

need to ensure that the total response in the cloud-locked experiment is similar to the response in the case with interactive clouds. As mentioned in the previous section, the mean CTL and 4xCO_2 climates may be different owing to the decorrelation between cloud, temperature, and moisture anomalies in the cloud-locked case. The differences in the responses to CO_2 quadrupling, shown in the right column of Fig. 1, are relatively small overall. The case with interactive clouds has very slightly larger surface warming (0.05 K global-mean difference), with the largest temperature differences

in the stratosphere and in the subtropics of the Northern Hemisphere. (Recall that since the model is hemispherically and zonally symmetric, any differences between the hemispheres are solely due to sampling error.) The slightly enhanced warming results in a modest enhancement of the poleward shift of the eddy-driven jet, particularly in the Northern Hemisphere, combined with a slight weakening of the subtropical jet core and an enhancement of the tropical superrotation. Differences in the mean meridional circulation response appear to be very small. We conclude that overall, the experiment

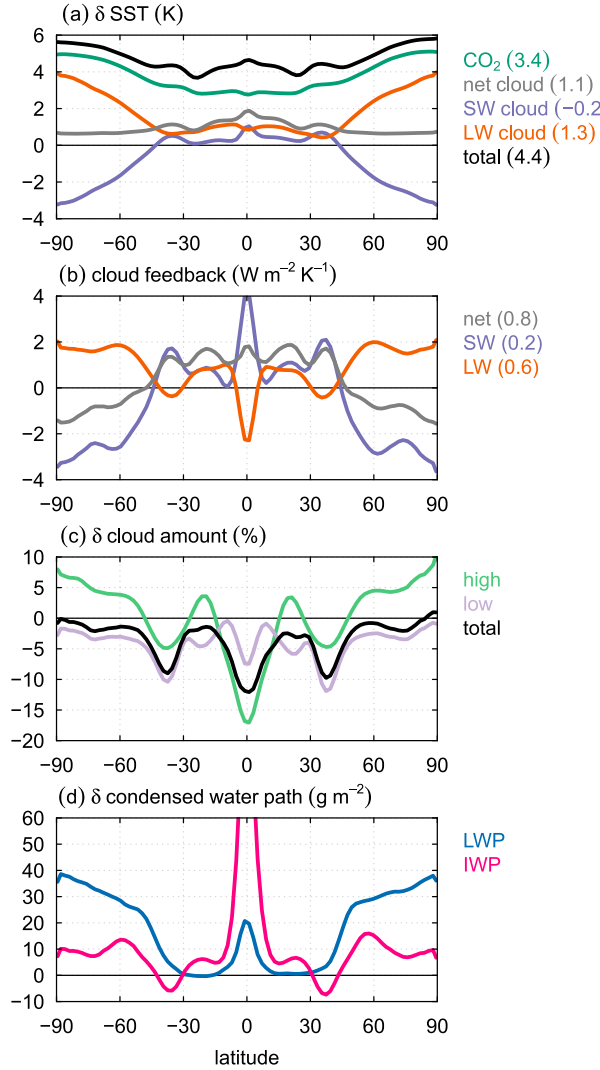


FIG. 2. (a) SST response broken down into effects of SW and LW cloud radiative changes and CO_2 forcing. (b) SW and LW cloud feedback. (c) High ($p < 440 \text{ hPa}$), low ($p > 680 \text{ hPa}$), and total cloud amount response. (d) Liquid and ice water path response. The cloud feedback in (b) is normalized by the total global-mean surface warming in the 4xCO_2 experiment including cloud changes (4.4 K).

with locked clouds provides a meaningful representation of the total climate response to CO_2 quadrupling in our model.

b. Surface temperature and cloud response

We next consider the breakdown of the SST response into cloud and CO_2 effects (Fig. 2a). Quadrupling CO_2 while holding the clouds fixed [Eq. (2)] causes a global-mean SST increase of 3.4 K, with the temperature change smoothly increasing with latitude from the tropics to the poles (green curve in Fig. 2a). As discussed in section 2, note that this response includes the effects

of the water vapor and lapse-rate feedbacks. While the ice-albedo feedback is not active in our simulations because of the absence of sea ice, amplified warming at high latitudes is still expected for several reasons. Temperature (Planck and lapse rate) feedbacks have been shown to drive polar amplification in CMIP5 models (Pithan and Mauritsen 2014), although the lapse-rate feedback is likely much weaker in our aqua-planet model given the lack of sea ice and associated low-level temperature inversions. But more importantly, even in the absence of local positive feedbacks, an increase in poleward energy transport by the atmosphere is to be expected in response to an increasing meridional moist static energy (MSE) gradient with warming, yielding enhanced energy convergence in polar regions (Hwang et al. 2011; Roe et al. 2015). The MSE gradient increase results from the larger increase in specific humidity at low latitudes, consistent with the Clausius–Clapeyron relationship under the assumption of near-constant relative humidity.

The SW cloud effect [Fig. 2a, purple curve; Eq. (3)] causes a negligible change in global-mean SST (-0.2 K) but features a strong latitude dependence, with a weak temperature increase in the tropics and lower mid-latitudes and strong cooling at high latitudes. The temperature response is in close agreement with the SW cloud feedback, shown in Fig. 2b (purple curve).¹ The negative SW cloud feedback at high latitudes results from increases in cloud water and optical depth rather than total cloud amount (Figs. 2c,d), consistent with most climate models (Zelinka et al. 2012, their Fig. 8b). The high-latitude cloud water increase is thought to be related to the effect of phase changes in mixed-phase clouds: warming favors a transition from ice to liquid water, reducing the overall precipitation efficiency and yielding an enhanced reservoir of cloud water (Senior and Mitchell 1993; Tushimura et al. 2006; McCoy et al. 2014a; Ceppi et al. 2015). In addition to the phase change effect, changes in the vertical derivative of the moist adiabat could also favor an increase in cloud water with warming, and this effect is most pronounced at lower temperatures (e.g., Betts and Harshvardhan 1987; Tselioudis et al. 1992). The resulting high-latitude cloud optical depth feedback is a very robust feature of global

¹The SW and LW cloud feedbacks were calculated in separate partial radiative perturbation (PRP) experiments, where the difference in radiative fluxes between instantaneous CTL and 4xCO_2 clouds was calculated at each time step. The radiative effect of cloud changes is the average of two PRP experiments, one with control CO_2 and one with quadrupled atmospheric CO_2 concentration, equivalent to a two-sided PRP (Colman and McAvaney 1997; Soden et al. 2008).

warming simulations in CMIP5 models (Zelinka et al. 2012; McCoy et al. 2014b; Ceppi et al. 2015). Most climate models also predict a positive SW cloud feedback in the tropics owing to cloud amount decreases (e.g., Bony and Dufresne 2005; Zelinka et al. 2012), although our physical understanding of these changes is more limited (Boucher et al. 2013). Thus, the overall structure of the SW cloud feedback in our model is consistent with the mean behavior of climate models, even though the strongly negative high-latitude feedback in our model causes a more negative global-mean SW cloud feedback compared to most models (Soden et al. 2008; Zelinka et al. 2012; Vial et al. 2013). As will be shown later in the paper, the increase in the meridional SST gradient caused by the SW cloud effect is a key component of the total response to CO₂ increase.

The temperature response due to the LW cloud effect [orange curve in Fig. 2a; Eq. (4)] mirrors the response to the SW effect, so that both effects partly cancel each other out. The LW cloud feedback largely reflects the high cloud amount response (Figs. 2b,c) and is positive in the global-mean, consistent with the rise of cloud tops under the fixed anvil temperature (FAT) hypothesis (Hartmann and Larson 2002; Zelinka and Hartmann 2010). The high cloud decreases in parts of the tropics are sufficiently large to offset the effect of rising cloud tops, yielding a negative feedback locally. The particularly strong positive LW cloud feedback at high latitudes is associated with very high cloud fraction in the control climate, especially at mid- and upper levels (not shown), yielding a strong LW effect of rising cloud tops. Despite the partial cancellation of SW and LW cloud radiative changes, the SST response to both cloud effects combined (gray curve) is still dominated by the SW effect in terms of the meridional structure, with peak warming at the equator and an overall increased equator-to-pole temperature gradient, while the global-mean SST increase results entirely from the LW effect of clouds.

c. Atmospheric circulation changes

We now study the vertical structure of changes in temperature and atmospheric circulation in our experiments. We begin by considering the zonal wind response and its relationship with temperature changes, shown in Fig. 3.

The CO₂ increase causes the expected tropospheric warming and stratospheric cooling, with warming maxima at upper levels in the tropics and in the lower polar troposphere (Fig. 3, top left). An interesting result is that increasing CO₂ while holding the clouds fixed causes very little change in the tropospheric jet (Fig. 3, top right). This result is surprising, since a poleward shift of the tropospheric eddy-driven jet is often regarded as one

of the most fundamental circulation responses to greenhouse gas forcing, especially in idealized models (Kushner et al. 2001; Yin 2005; Brayshaw et al. 2008; Lu et al. 2010). The zonal wind response mainly consists of an upward shift of the jet stream, consistent with the troposphere becoming warmer and deeper. A slight weakening of the tropospheric jet is seen on the equatorward flank of the jet at the lowest levels, resulting in a poleward jet shift of 0.9° (based on the latitude of peak zonal-mean zonal wind at the surface, cubically interpolated onto a 0.1° grid). The relatively modest poleward jet shift in the troposphere appears consistent with the structure of the temperature response: while at upper levels the warming peaks in the tropics, in the lower troposphere it maximizes at high latitudes, a result consistent with previous modeling evidence (e.g., Held 1993). Upper-level tropical warming and lower-level polar warming have been shown to have opposing influences on the eddy-driven jet response (Butler et al. 2010).

By contrast, the relatively modest temperature response caused by the SW cloud feedback produces a substantial zonal wind response in the troposphere, with a clear strengthening and poleward shift of the eddy-driven jet (Fig. 3, second row). As will be shown below, the large eddy-driven jet response is related to the spatial structure of the thermal forcing associated with the SW cloud feedback, which causes an enhancement of the meridional temperature gradient at all levels in the troposphere. The fact that an increased mid-latitude temperature gradient tends to favor a poleward jet shift has been noted in several previous studies (Brayshaw et al. 2008; Chen et al. 2010; Ceppi et al. 2012; Lorenz 2014). While the mechanisms of the eddy-driven jet response to thermal forcing are still a topic of active research, our results appear consistent with several existing theories. Lorenz (2014) proposed that stronger upper-level westerlies near the jet result in changes in Rossby wave propagation, favoring a poleward shift of the region of eddy momentum flux convergence. Chen and Held (2007) argued that increasing eddy phase speeds could cause a poleward shift of the eddy-driven circulation; an eddy phase speed increase could occur in response to a strengthened meridional temperature gradient and upper-level westerly winds. Besides the poleward jet shift, we also note a transition to more westerly winds in the upper tropical troposphere, which are sustained by enhanced eddy momentum flux convergence associated with tropical waves (not shown).

Unlike the effect of SW cloud radiative changes, the LW effect yields a tropospheric temperature response qualitatively similar to that of CO₂, but weaker overall and with a higher degree of polar amplification at low

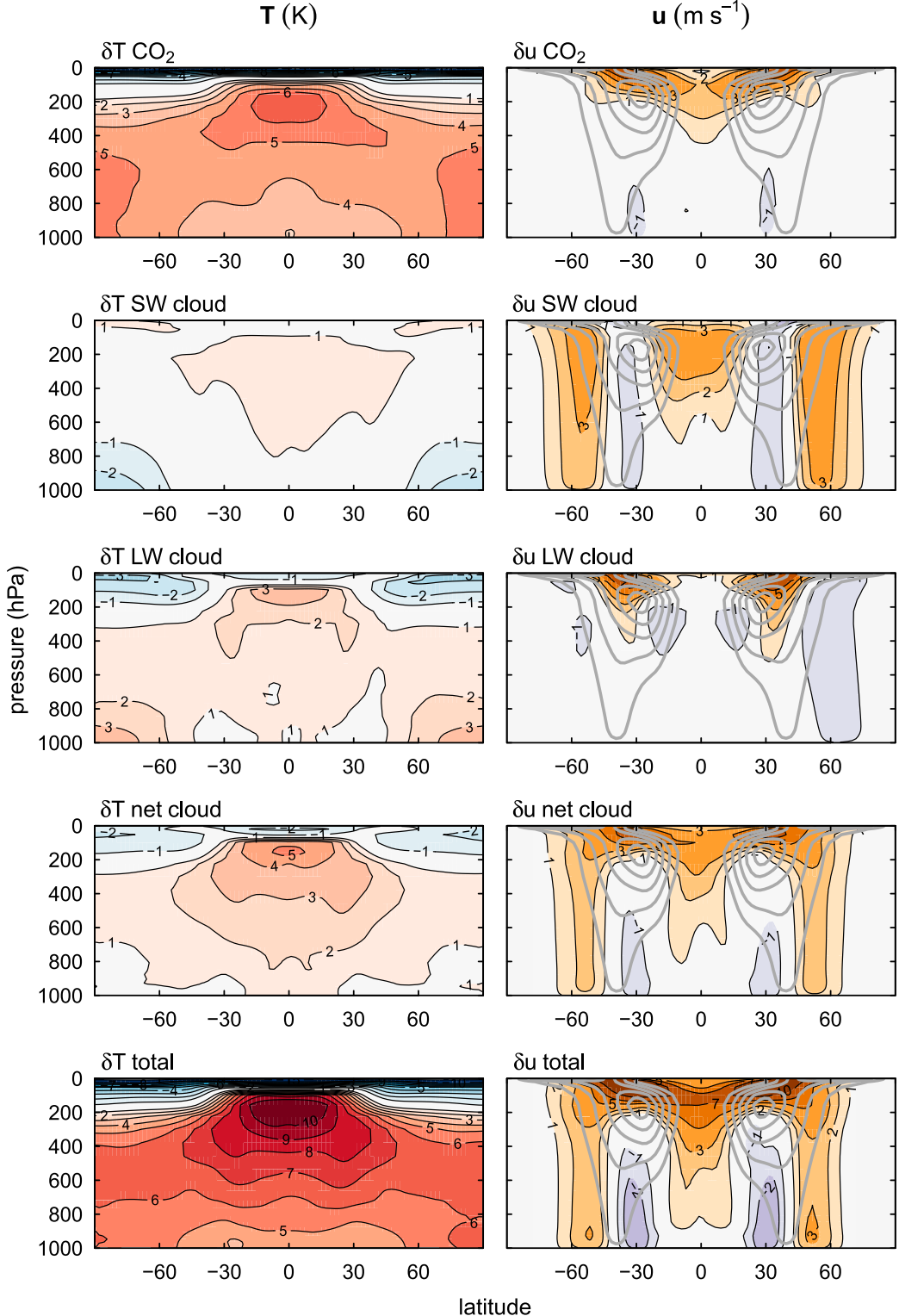


FIG. 3. (left) Temperature and (right) zonal wind responses to CO_2 quadrupling, broken down into contributions from CO_2 forcing and clouds. Shading denotes the response. In the right column, thick gray contours represent the control climatology (contour interval $10 m s^{-1}$, only positive values shown). The CO_2 , SW cloud, and LW cloud effects are calculated with Eqs. (2), (3), and (4), respectively.

levels (Fig. 3, third row). Like CO₂, this forcing also mainly causes an upward shift of the jet streams, with a relatively weak tropospheric response that occurs mostly above 500 hPa and resembles a narrowing of the westerly jet.

Adding the SW and LW cloud responses together yields the net effect of cloud radiative changes (fourth row of Fig. 3), consisting of generalized tropospheric warming peaking in the tropical upper troposphere. It is noteworthy that the net cloud effect results in a warming pattern quite different from CO₂ forcing, with an increase in equator-to-pole temperature gradient at all tropospheric levels. The temperature change due to clouds yields a clear poleward and upward shift of the tropospheric jet. Finally, the total response to CO₂ quadrupling, including the effects of cloud changes, is shown in the bottom row of Fig. 3; recall that this response is identical to the sum of rows 1–3, by construction. The tropospheric zonal wind response most resembles the effect of clouds (cf. rows 4 and 5). The large contribution of cloud radiative changes to the tropospheric circulation response will be confirmed later in this paper, using various metrics to objectively quantify circulation shifts.

The very distinct effects of cloud radiative changes and CO₂ forcing on the thermal structure of the troposphere are summarized in Fig. 4. To quantify the overall change in tropospheric thermal structure at various levels, we define the mean upper- and lower-tropospheric temperature as the vertically averaged values from 100 to 500 hPa and 500 to 1000 hPa, respectively, which we denote as $\langle T \rangle_{\text{upper}}$ and $\langle T \rangle_{\text{lower}}$ (Figs. 4a,c). In the upper troposphere, both clouds and CO₂ forcing cause enhanced tropical warming, yielding an enhanced thermal gradient between the tropics (30°S–30°N) and the extratropics (Figs. 4a,b). Both the SW and LW cloud changes contribute to the enhanced upper-tropospheric temperature gradient, even though the LW effect is almost twice as large. In the lower troposphere, however, only the SW cloud radiative changes act to enhance the meridional temperature gradient, while both the LW cloud effect and CO₂ forcing cause polar-amplified warming (Figs. 4c,d). Thus, *in a tropospheric-mean sense* the SW cloud radiative change is the main contributor to the amplified temperature gradient; while CO₂ forcing and LW cloud radiative changes yield substantial warming, they cause negligible change in the gradient of tropospheric temperature in the vertical mean (Figs. 4e,f). This result strongly suggests that the change in temperature gradient at all tropospheric levels is much more relevant to the atmospheric circulation response than the change in mean temperature, at least in terms of the poleward expansion of the circulation.

We next assess changes in eddy activity, measured by the eddy kinetic energy (EKE) as $\text{EKE} = (\bar{u}^2 + \bar{v}^2)/2$, where primes denote deviations from the zonal and time mean and overbars indicate zonal and time averages (left column of Fig. 5). Around the midlatitudes, EKE provides a measure of the location and intensity of the storm track, which modulates important climate properties in the extratropics such as cloudiness and precipitation. Comparing with the temperature changes in Fig. 3, we find that the tropospheric EKE response is strongly tied to changes in the meridional temperature gradient, consistent with the idea that baroclinicity is the dominant control on eddy activity. The largest tropospheric response is an increase and poleward shift of EKE caused by the SW cloud feedback in midlatitudes, but it is opposed by weaker EKE decreases by the LW cloud feedback and CO₂ forcing with clouds fixed, resulting in a near-zero total response below 200 hPa (Fig. 5, bottom left). The total EKE response mainly consists of an upward expansion in midlatitudes (consistent with the deepening of the troposphere with warming), as well as a strengthening of eddy activity around the equatorial tropopause, which results mainly from the CO₂ and SW cloud effects.

Finally, we discuss the response of the meridional mass streamfunction (calculated as $\Psi = 2\pi a g^{-1} \int_0^{p_0} \bar{v} \cos\phi \, dp$, where a is the radius of the Earth, g is gravitational acceleration, \bar{v} is zonal-mean meridional wind, ϕ is latitude, p is pressure, and p_0 is surface pressure). The mass streamfunction reflects the Hadley circulation climatology, which is an important control on the moisture budget in the intertropical convergence zone (ITCZ) and in subtropical dry regions (Hartmann 1994). Overall, the mass streamfunction response consists of a weakening of the Hadley circulation, except in the response to SW cloud radiative changes (right column of Fig. 5). The Hadley cell response to various forcings appears consistent with the competing effects of increasing meridional SST gradient and increasing static stability. While the SW effect tends to enhance the meridional SST gradient within the tropics, favoring a strengthening of the circulation, cloud changes also yield a stabilization of the tropics, especially through the LW effect, which favors a Hadley cell weakening (Knutson and Manabe 1995; Gastineau et al. 2008). This results in a very small overall change in Hadley cell strength in response to the net cloud radiative changes. In the case of CO₂ quadrupling with fixed clouds, tropical SST gradients change little (Fig. 2a) and the stability increase dominates, resulting in a marked weakening of the Hadley circulation.

A modest poleward expansion of the Hadley cell edge also occurs in response to each of the forcings; while this response is too weak to be visible in the responses to individual forcings, it appears clearly in the total

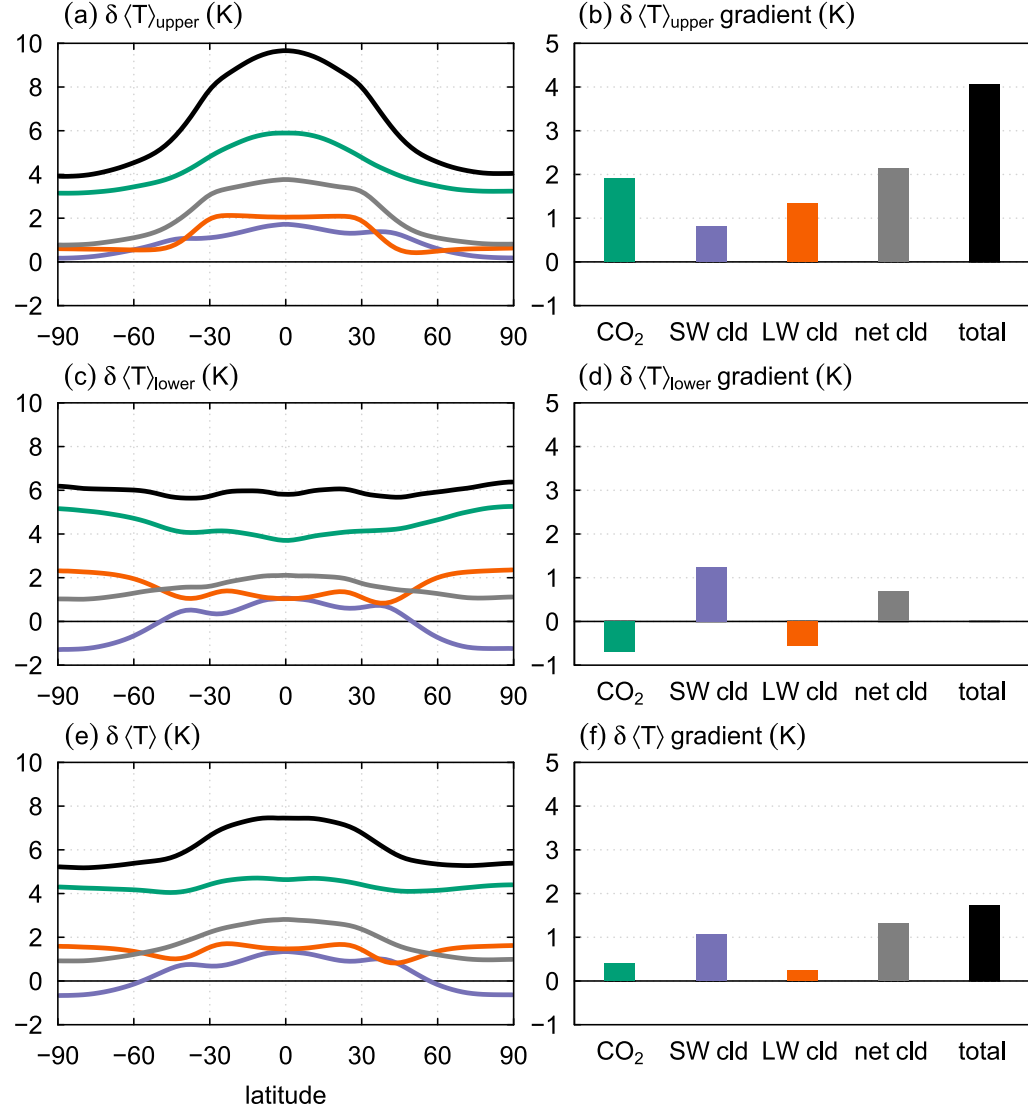


FIG. 4. (a),(c),(e) As in Fig. 2a, but showing the response of the vertically averaged tropospheric temperature. Variables $\langle T \rangle_{\text{upper}}$, $\langle T \rangle_{\text{lower}}$, and $\langle T \rangle$ denote upper-tropospheric (100–500 hPa), lower-tropospheric (500–1000 hPa), and tropospheric (100–1000 hPa) vertical-mean temperature, respectively. (b),(d),(f) Changes in the meridional gradient of $\langle T \rangle$ at various tropospheric levels, calculated as the change in tropical mean $\langle T \rangle$ (30°S – 30°N) minus the change in extratropical mean $\langle T \rangle$.

streamfunction response (Fig. 5, bottom right). The poleward shift of the Hadley cell edge may result from the combined influences of the stabilization of the tropical troposphere, which shifts the latitudes of baroclinic instability poleward (Frierson et al. 2007; Lu et al. 2007), and from changes in the wave driving of the circulation. For example, increases in Rossby wave phase speeds with global warming (Chen and Held 2007) could cause a poleward shift of eddy momentum flux divergence and associated subtropical wave breaking, driving an anomalous meridional circulation consistent with a Hadley cell expansion (Ceppi and Hartmann

2013; Vallis et al. 2014). The Hadley cell weakening and poleward expansion are robust features of the atmospheric circulation response to warming (Frierson et al. 2007; Lu et al. 2007; Gastineau et al. 2008; Ceppi and Hartmann 2013; Vallis et al. 2014).

d. Poleward expansion of the atmospheric circulation

We have shown that cloud feedbacks with global warming produce thermal forcings that are particularly effective at inducing a poleward expansion of the tropospheric circulation in our aquaplanet model, particularly through the impact of SW cloud radiative changes

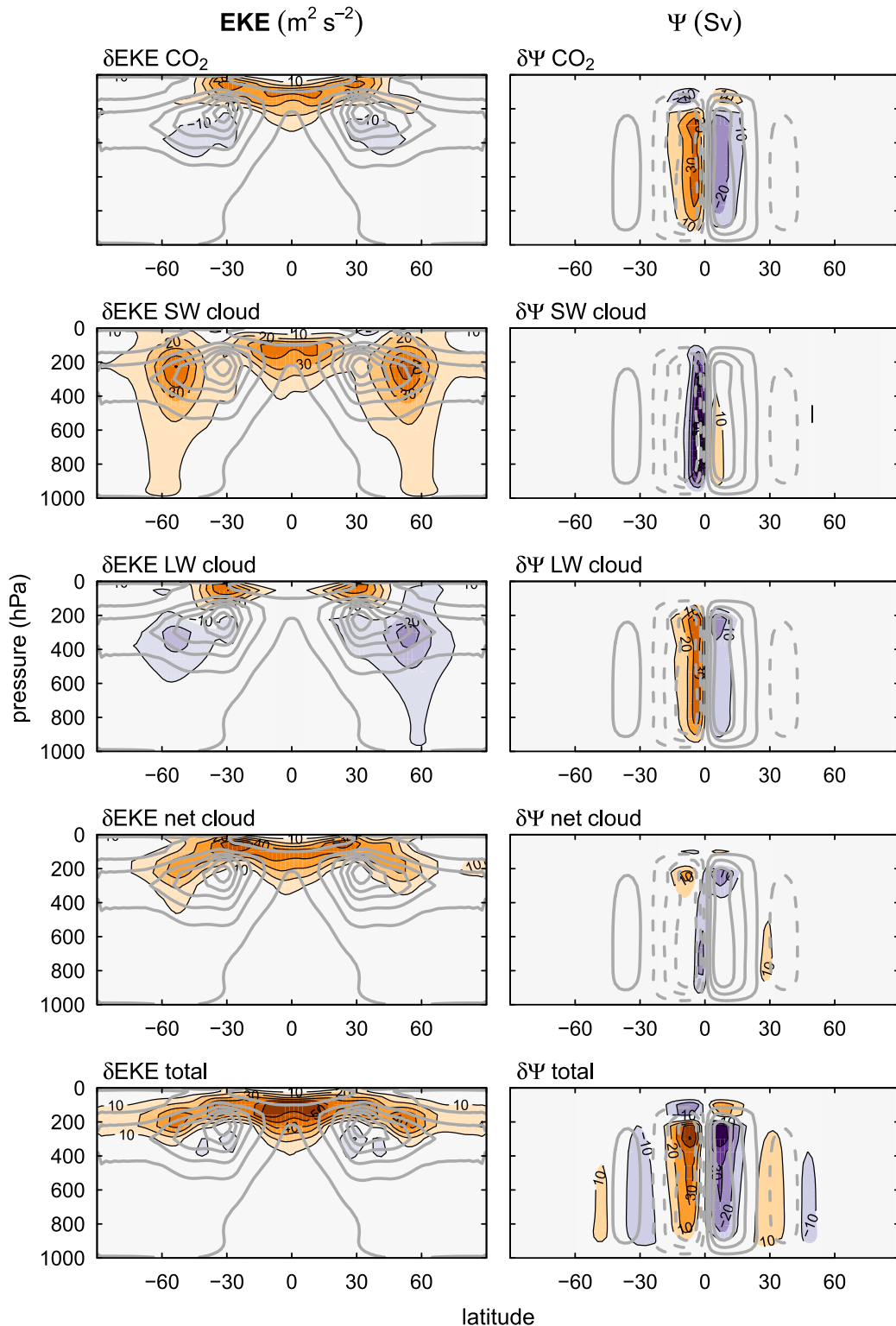


FIG. 5. As in Fig. 3, but for (left) EKE and (right) meridional mass streamfunction (Ψ). Gray contours show the control climatology in intervals of $40 \text{ m}^2 \text{s}^{-2}$ (EKE) and 60 Sv (Ψ), with negative values dashed and the zero contour omitted.

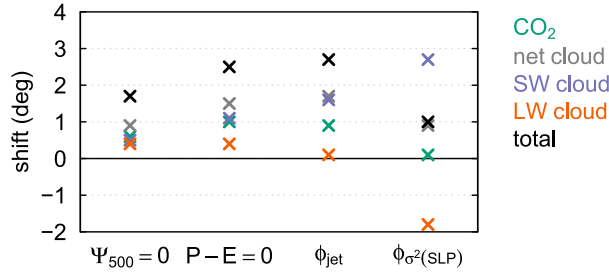


FIG. 6. The $4\times\text{CO}_2$ response of various circulation metrics: Hadley cell edge defined as the first zero-crossing of the mass streamfunction at 500 hPa ($\Psi_{500} = 0$), latitude where precipitation equals evaporation in the subtropics ($P - E = 0$), jet latitude defined as the peak in surface zonal-mean zonal wind (ϕ_{jet}), and storm-track latitude defined as the peak in SLP variance ($\phi_{\sigma^2(\text{SLP})}$). All results are averaged over both hemispheres.

on meridional temperature gradients. To objectively quantify the contribution of clouds to the expansion of the circulation, we calculate changes in four circulation metrics: the poleward edge of the Hadley circulation based on the meridional mass streamfunction at 500 hPa; the edge of the subtropical dry zones, calculated as the latitude where precipitation equals evaporation in the subtropics ($P - E = 0$); the jet latitude measured as the peak surface zonal-mean zonal wind; and the latitude of the storm tracks, measured as the peak in sea level pressure (SLP) variance. For each of these metrics, the fields of interest are cubically interpolated onto a 0.1° grid before locating the latitudes. For storm-track latitude, we use SLP variance rather than EKE for consistency with previous studies (e.g., Chang et al. 2012; Harvey et al. 2014); however, note that the results are similar if surface EKE is used instead. As in Harvey et al. (2014), we use 2–6-day bandpass-filtered SLP data to quantify the variability associated with transient synoptic eddies.

The changes in each of the metrics relative to the control climate are shown in Fig. 6. Both clouds and CO_2 forcing alone contribute to the expansion of the tropics, as measured by the edge of the Hadley cells and of the subtropical dry zones. However, their impacts on the jet and storm-track position are very different, with SW cloud radiative changes having the largest positive effect. The strong SW cloud effect on jet and storm-track latitude is consistent with the zonal wind and EKE responses shown in Figs. 3 and 5. It is noteworthy that the storm-track latitude is much more sensitive to SW and LW cloud effects than is the jet position; this may be related to the much higher climatological latitude of the storm track compared to the jet, as defined here (52.4° versus 38.9°), making the storm track more responsive to high-latitude temperature changes. Remarkably, in our model the SW radiative response associated with clouds

TABLE 1. Hemispherically averaged latitudinal shift in various atmospheric circulation metrics, with poleward shifts defined as positive. The CTL latitude is provided in the second row for reference. For a definition of the metrics, see Fig. 6 and text. The symbols used for the experiments are described in section 2. The mean CO_2 , SW cloud, and LW cloud effects are calculated as in Eqs. (2)–(4).

Experiment	$\Psi_{500} = 0$	$P - E = 0$	ϕ_{jet}	$\phi_{\sigma^2(\text{SLP})}$
CTL	26.7	35.2	38.9	52.4
G2S1L1 – G1S1L1	0.8	1.1	1.4	0.1
G2S2L2 – G1S2L2	0.5	0.9	0.5	0.1
Mean CO_2 effect	0.6	1.0	0.9	0.1
G1S2L1 – G1S1L1	0.9	1.5	2.5	1.9
G1S2L2 – G1S1L2	0.2	0.8	1.0	3.1
G2S2L1 – G2S1L1	0.6	1.2	1.9	4.6
G2S2L2 – G2S1L2	0.2	1.0	1.1	1.4
Mean SW cloud effect	0.5	1.1	1.6	2.7
G1S1L2 – G1S1L1	0.8	0.8	0.9	-2.4
G1S2L2 – G1S2L1	0.1	0.3	-0.2	-1.2
G2S1L2 – G2S1L1	0.5	0.4	0.1	-2.0
G2S2L2 – G2S2L1	0.1	0.3	-0.3	-1.5
Mean LW cloud effect	0.4	0.4	0.1	-1.8

is the only factor contributing to the poleward shift of the storm track. The net effect of cloud feedbacks is to force a poleward expansion of the circulation that strongly enhances the effect of CO_2 forcing, while the CO_2 increase only yields only a modest circulation shift if the clouds are held fixed. This result becomes clear by comparing the gray and black crosses in Fig. 6, which show that the cloud radiative changes explain more than half of the total expansion of the circulation.

As described in Eqs. (2)–(4), the responses to each of the forcings result from averages over several experiments. Comparing the responses to a particular forcing across experiments provides a measure of the sensitivity of the response to the reference climate. The shifts in each of the circulation metrics shown in Fig. 6 are listed in Table 1 for all experiments. For each individual forcing, there are clear differences in the magnitude of the shift in each of the metrics between experiments. Part of these differences may result from random internal variability, but we believe most of the differences reflect a sensitivity to the initial climate. Despite this nonlinear behavior, the effect of each forcing on atmospheric circulation remains qualitatively consistent across experiments. For example, for each metric and forcing, the sign of the shift is identical across all experiments; the only exception is the eddy-driven jet response to LW cloud changes, which is generally close to zero.

4. Discussion

The main purpose of this paper is to show that cloud feedbacks produce thermal forcings that can substantially

alter the large-scale circulation response to CO₂ increase. Our results support the finding of Ceppli et al. (2014), of a strong relationship between the meridional structure of SW feedbacks and the austral jet stream response in CMIP5 models under RCP8.5 forcing. They are also consistent with the large effect of clouds on the mean circulation shown by Li et al. (2015). Recently, Voigt and Shaw (2015) demonstrated the importance of cloud and water vapor feedbacks on the circulation response in two aquaplanet models forced with a uniform SST increase. Because the SSTs are prescribed, however, it is likely that their results mainly reflect the effect of LW cloud feedbacks, since SW radiation is mostly absorbed at the surface. A novel aspect of our study is the separate consideration of SW and LW cloud feedbacks, which highlights the important but different roles of SW and LW cloud effects when SSTs are allowed to interact with radiation.

a. Cloud feedbacks in contemporary climate models

Care must be taken in generalizing our results to other models, for at least two reasons. First and foremost, cloud feedbacks are highly uncertain and model dependent, and so is their effect on atmospheric circulation. To quantify their contribution to the mean and spread in atmospheric circulation changes with warming, it is therefore necessary to test the effects of cloud changes in a wider set of models. Despite this uncertainty, we will argue below that the meridional structures of the SW and LW cloud feedbacks produced by our model are fairly representative of the mean behavior of state-of-the-art climate models. Second, our experiment design is highly idealized. The low surface albedo associated with the aquaplanet configuration may lead to an overestimation of the SW effect of clouds, particularly compared with Northern Hemisphere conditions. The sensitivity of the atmospheric circulation to external forcings may be overestimated given the low climatological jet latitude in our model (38.9°), especially compared to the Southern Hemisphere (Kidston and Gerber 2010). Also, the zonally symmetric boundary conditions mean that stationary waves play no role in the atmospheric circulation response to CO₂ forcing, unlike the real world (Simpson et al. 2014). However, the idealized experimental design also allows for an easier interpretation of the basic effects of cloud feedbacks on circulation.

Cloud feedbacks play a special role in the atmospheric circulation response to warming for two reasons: 1) they tend to enhance the equator-to-pole temperature gradient and midlatitude baroclinicity and 2) they are highly uncertain and cause intermodel spread in circulation changes. Figure 7, showing the cloud feedback

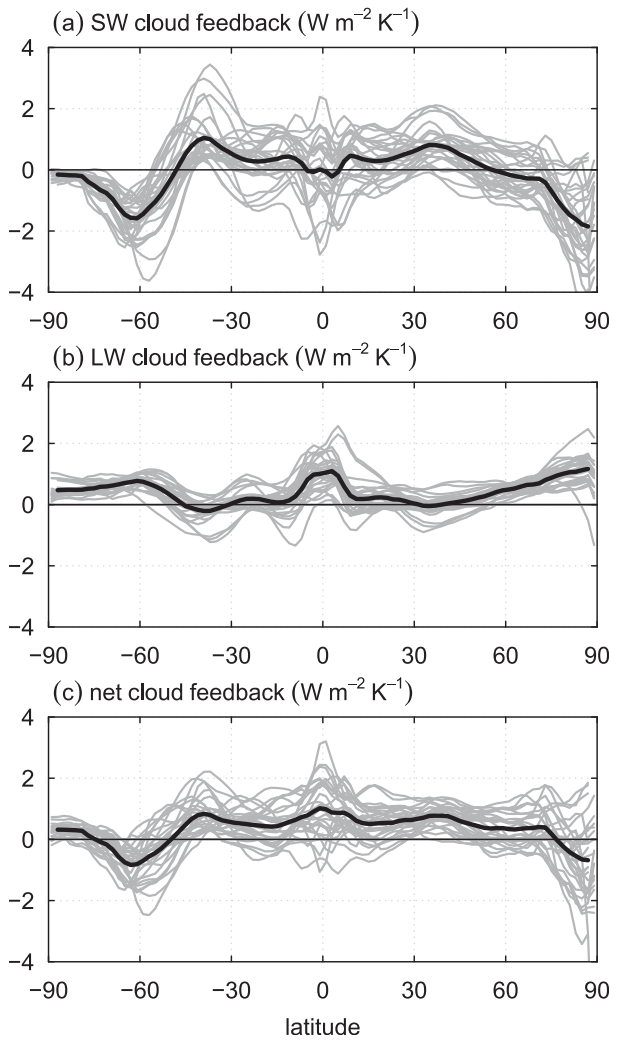


FIG. 7. Cloud feedback components in the abrupt4xCO₂ experiment of 28 CMIP5 models, all calculated as years 121–140 minus the preindustrial control climatology. Gray curves represent individual models, with the multimodel mean as the thick black line. The cloud feedback is calculated using radiative kernels, following the method of Soden et al. (2008), and includes rapid adjustments to CO₂ forcing (Sherwood et al. 2015).

components in the abrupt4xCO₂ simulations of 28 CMIP5 models, illustrates these two points. As in our idealized model, the mean SW cloud feedback in CMIP5 models leads to an overall enhanced meridional gradient of absorbed SW radiation around the midlatitudes, with a positive mean feedback in the tropics and a negative feedback at high latitudes. By contrast, the LW cloud feedback tends to be positive at all latitudes. Because the LW cloud feedback has less spatial structure than the SW feedback, the net feedback is dominated by the SW component (Fig. 7c), tending to enhance the meridional gradient of absorbed SW radiation; this is also in agreement with our model results (see Fig. 2b).

Comparing the gray curves in [Fig. 7](#) provides an idea of the uncertainty in the magnitude and spatial distribution of the cloud feedbacks, which is particularly large for the SW component.

b. Relationship between feedback and temperature response

Intermodel differences in cloud feedbacks motivate a discussion of the relationship between the meridional structure of the feedbacks and the structure of the resulting temperature response. It is important to recognize that changes in top-of-atmosphere radiation associated with feedbacks do not necessarily predict the meridional structure of the associated temperature change, owing to the role of meridional energy transport ([Langen et al. 2012](#); [Merlis 2014](#)), consistent with climate feedbacks being fundamentally nonlocal in nature ([Feldl and Roe 2013](#)). With this complication in mind, how robust are our results to variations in the spatial pattern of the SW and LW cloud feedbacks?

The strong poleward circulation shift induced by the SW cloud feedback relies on an overall enhancement of the tropospheric meridional temperature gradient. If the tropical SW cloud feedback is positive as most models predict, the resulting increase in tropical MSE will induce an enhancement of the poleward energy transport by the atmosphere, causing polar-amplified warming unless the high-latitude SW cloud feedback is sufficiently negative. In other words, the SW cloud feedback could produce polar amplification at low levels even if the equator-to-pole gradient of absorbed SW radiation is enhanced. The remote effects of tropical climate feedbacks on the high-latitude temperature response are clearly illustrated in Fig. 2 of [Roe et al. \(2015\)](#). The circulation impacts of the SW cloud feedback would likely also depend on the degree of tropical upper-tropospheric warming, which we expect to be directly linked to the amount of tropical SST increase caused by SW cloud radiative changes, since surface and upper-tropospheric temperatures are tightly coupled in the tropics through the effects of convection.

Thus, the net effect of the SW cloud feedback on circulation is determined by the relative magnitudes of the positive tropical forcing and negative high-latitude forcing; for example, we would expect to find a much weaker poleward expansion of the circulation by the SW cloud feedback in a model in which this feedback is much less negative at high latitudes. While the negative SW cloud feedback at high latitudes is a robust feature of CMIP5 global warming experiments ([Fig. 7a](#)) and is supported by a robust physical mechanism (phase changes in mixed-phase clouds; [section 3b](#)), the magnitude of this negative high-latitude feedback—both in

absolute terms and relative to the generally positive SW cloud feedback in the tropics—is highly model dependent.

We believe the temperature and circulation impacts of the LW cloud feedback are somewhat more robust. In presence of a positive LW cloud feedback at most latitudes, the low-level temperature response to LW cloud radiative changes is very likely to be amplified at high latitudes owing to the effect of increasing meridional energy transport and positive temperature feedbacks ([Pithan and Mauritsen 2014](#); [Roe et al. 2015](#)). An overall positive LW cloud feedback is expected as cloud tops rise with warming, consistent with the FAT hypothesis ([Hartmann and Larson 2002](#)); models agree on this effect, and there is no physical argument to expect a negative LW cloud feedback at high latitudes. However, the degree of polar amplification at low levels will still be affected by the magnitude of the local LW cloud feedback. In our model, the high-latitude LW cloud feedback appears too positive, which we ascribe to an unrealistically high climatological cloud fraction in our aquaplanet configuration in high latitudes ([section 3b](#)). It is therefore possible that our model overestimates the amount of polar amplification associated with the LW cloud feedback and therefore underestimates the contribution of LW cloud radiative changes on the poleward expansion of the circulation, compared to more realistic models.

Despite the complex relationship between feedback patterns and temperature responses, [Ceppi et al. \(2014\)](#) showed that the meridional structure of SW feedbacks (mainly from clouds and sea ice) explains the changes in SST gradient very well in RCP8.5 simulations around the southern midlatitudes. From the perspective of the atmospheric circulation response, the results in the present paper suggest that the spatial distribution of the thermal forcing, both at lower- and upper-tropospheric levels, is more important than the global-mean effect, as discussed in [section 4a](#). Hence, the results in [Fig. 7](#) support the idea that the cloud feedback likely enhances the poleward expansion of atmospheric circulation in most climate models.

c. Effects of other climate feedbacks

While the focus of this paper has been on the effects of clouds, other feedbacks will also affect the temperature and circulation responses to greenhouse gas forcing in climate models. For example, the large-scale effects of the water vapor feedback have been demonstrated in previous studies ([Schneider et al. 1999](#); [Hall and Manabe 1999](#); [Mauritsen et al. 2013](#); [Voigt and Shaw 2015](#)). Although [Voigt and Shaw \(2015\)](#) found an equatorward contraction of the atmospheric circulation

in response to radiative changes of water vapor, it is not obvious that a similar response would be obtained in a coupled atmosphere–ocean climate model like ours. This is because water vapor changes cause a very different temperature response when SSTs are allowed to respond to the radiative forcing, with substantial warming in the tropical upper troposphere (cf. Fig. 6d in Langen et al. 2012 with Fig. 3c in Voigt and Shaw 2015). Furthermore, since the water vapor content is so strongly tied to temperature through the Clausius–Clapeyron relationship, we speculate that the uncertainty in the circulation response associated with the water vapor feedback is much smaller than that caused by cloud changes.

By contrast, we believe that the temperature and surface albedo feedbacks could contribute significant uncertainty to the spatial pattern of the temperature increase and the associated circulation response in climate models. Temperature feedbacks (including the Planck and lapse-rate feedbacks) have been shown to contribute to polar warming (Pithan and Mauritsen 2014). The lapse-rate feedback, which is the strongest contribution to Arctic warming in CMIP5 models (Pithan and Mauritsen 2014), is positive at high latitudes because of the existence of strong low-level inversions that trap warming near the surface. It is therefore plausible that the lapse-rate feedback in high latitudes could depend on the strength of the polar low-level inversions in the control climate. Finally, the surface albedo feedback is dominated by fairly uncertain changes in sea ice extent and snow cover, and while its effect on global-mean temperature is much smaller than that of cloud feedbacks (Vial et al. 2013), it has a strong effect on polar amplification in CMIP5 models (Pithan and Mauritsen 2014).

5. Summary and conclusions

This paper investigates the effect of cloud feedbacks on the atmospheric circulation response to CO₂ quadrupling in an aquaplanet model with a slab ocean lower boundary. We use a cloud-locking technique to break down the circulation response into two main components: the response to CO₂ increase while clouds are fixed and the response to cloud changes while CO₂ is fixed. The response to cloud changes is further decomposed into SW and LW cloud effects. We find that cloud changes cause a very substantial atmospheric circulation response, inducing a poleward expansion of the Hadley cells, midlatitude jet streams, and storm tracks. This response is dominated by the SW effect of clouds, while LW cloud radiative changes alone force a modest tropical expansion, no jet shift, and an equatorward shift of the storm tracks.

While quadrupling CO₂ with fixed clouds also forces an expansion of the circulation, this effect is smaller than the net effect of cloud changes, despite the fact that CO₂ quadrupling causes 3 times as much surface warming than cloud changes in the global mean (3.4 versus 1.1 K). We explain this surprising result in terms of the spatial structures of the thermal forcings associated with CO₂ and cloud radiative changes. The SW effect of cloud changes is to strongly enhance the equator-to-pole temperature gradient at all tropospheric levels, increasing midlatitude baroclinicity. Previous research has associated this type of forcing with a clear strengthening and poleward shift of the jet streams and storm tracks. By contrast, the CO₂ increase (and to a lesser extent the LW cloud radiative changes) causes global warming with peak warming in low-level polar regions and in the upper tropical troposphere. We believe that the different changes in meridional temperature gradient at upper and lower levels have opposing effects on atmospheric circulation, reducing the impact of these forcings on the expansion of the circulation.

Our results highlight the importance of the spatial structure of the temperature response as opposed to the global-mean response, since the SW cloud radiative changes cause the smallest global-mean surface temperature change (−0.2 K), but the largest midlatitude circulation response in our model. Thus, it is important to note that clouds could enhance the atmospheric circulation response to CO₂ forcing even in a hypothetical case where the global-mean cloud feedback is near-zero or negative. This suggests that in terms of large-scale circulation impacts, changes in meridional temperature gradients may be at least as important as the amount of global-mean warming.

We caution that the results presented in this paper are based on a single model and are not necessarily representative of the atmospheric circulation impacts of cloud feedbacks in other models or in the real world. However, an analysis of the cloud feedbacks in CMIP5 model experiments with quadrupled CO₂ concentrations reveals that the key basic features of the cloud radiative response are similar to our model—particularly the tendency of cloud feedbacks to enhance the equator-to-pole temperature gradient through the SW effect. We therefore argue that cloud changes likely enhance the poleward expansion of the circulation with global warming in most state-of-the-art climate models. Because of the large uncertainty in the cloud response, it is also likely that clouds significantly contribute to intermodel differences in the atmospheric circulation response, as suggested by previous research (Ceppi et al. 2014; Voigt and Shaw 2015).

This study has focused on the atmospheric circulation response mainly from the perspective of the poleward expansion of the Hadley cells, jet streams, and storm tracks, in an idealized, zonally and hemispherically symmetric setting. In a more realistic configuration, cloud feedbacks would likely also have an important effect on the asymmetric component of the circulation, impacting the amplitude and location of stationary waves (Donner and Kuo 1984; Slingo and Slingo 1988) as well as interhemispheric asymmetries and the latitude of the intertropical convergence zone (Frierson and Hwang 2012). This further underlines the fact that constraining cloud feedbacks is essential not only for an accurate estimation of climate sensitivity, but also for a realistic representation of the atmospheric circulation response to greenhouse gas forcing.

Acknowledgments. The authors thank Dave Thompson and anonymous reviewers for their helpful comments on the manuscript, as well as Gerard Roe for discussion of the results. This work was supported by the National Science Foundation under Grant AGS-09604970. We also acknowledge the World Climate Research Programme's Working Group on Coupled Modelling, which is responsible for CMIP, and we thank the climate modeling groups for producing and making available their model output. For CMIP, the U.S. Department of Energy's Program for Climate Model Diagnosis and Intercomparison provides coordinating support and led development of software infrastructure in partnership with the Global Organization for Earth System Science Portals.

REFERENCES

Barnes, E. A., and L. Polvani, 2013: Response of the midlatitude jets, and of their variability, to increased greenhouse gases in the CMIP5 models. *J. Climate*, **26**, 7117–7135, doi:10.1175/JCLI-D-12-00536.1.

Betts, A. K., and Harshvardhan, 1987: Thermodynamic constraint on the cloud liquid water feedback in climate models. *J. Geophys. Res.*, **92**, 8483–8485, doi:10.1029/JD092iD07p08483.

Bony, S., and J.-L. Dufresne, 2005: Marine boundary layer clouds at the heart of tropical cloud feedback uncertainties in climate models. *Geophys. Res. Lett.*, **32**, L20806, doi:10.1029/2005GL023851.

Boucher, O., and Coauthors, 2013: Clouds and aerosols. *Climate Change 2013: The Physical Science Basis*, T. F. Stocker et al., Eds., Cambridge University Press, 571–657.

Brayshaw, D. J., B. Hoskins, and M. Blackburn, 2008: The storm-track response to idealized SST perturbations in an aqua-planet GCM. *J. Atmos. Sci.*, **65**, 2842–2860, doi:10.1175/2008JAS2657.1.

Butler, A. H., D. W. J. Thompson, and R. Heikes, 2010: The steady-state atmospheric circulation response to climate change-like thermal forcings in a simple general circulation model. *J. Climate*, **23**, 3474–3496, doi:10.1175/2010JCLI3228.1.

Caballero, R., and M. Huber, 2010: Spontaneous transition to superrotation in warm climates simulated by CAM3. *Geophys. Res. Lett.*, **37**, L11701, doi:10.1029/2010GL043468.

Ceppi, P., and D. L. Hartmann, 2013: On the speed of the eddy-driven jet and the width of the Hadley cell in the Southern Hemisphere. *J. Climate*, **26**, 3450–3465, doi:10.1175/JCLI-D-12-00414.1.

—, Y.-T. Hwang, D. M. W. Frierson, and D. L. Hartmann, 2012: Southern Hemisphere jet latitude biases in CMIP5 models linked to shortwave cloud forcing. *Geophys. Res. Lett.*, **39**, L19708, doi:10.1029/2012GL053115.

—, M. D. Zelinka, and D. L. Hartmann, 2014: The response of the Southern Hemispheric eddy-driven jet to future changes in shortwave radiation in CMIP5. *Geophys. Res. Lett.*, **41**, 3244–3250, doi:10.1002/2014GL060043.

—, D. L. Hartmann, and M. J. Webb, 2015: Mechanisms of the negative shortwave cloud feedback in middle to high latitudes. *J. Climate*, doi:10.1175/JCLI-D-15-0327.1, in press.

Chang, E. K. M., Y. Guo, and X. Xia, 2012: CMIP5 multimodel ensemble projection of storm track change under global warming. *J. Geophys. Res.*, **117**, D23118, doi:10.1029/2012JD018578.

Chen, G., and I. M. Held, 2007: Phase speed spectra and the recent poleward shift of Southern Hemisphere surface westerlies. *Geophys. Res. Lett.*, **34**, L21805, doi:10.1029/2007GL031200.

—, R. A. Plumb, and J. Lu, 2010: Sensitivities of zonal mean atmospheric circulation to SST warming in an aqua-planet model. *Geophys. Res. Lett.*, **37**, L12701, doi:10.1029/2010GL043473.

Colman, R. A., and B. J. McAvaney, 1997: A study of general circulation model climate feedbacks determined from perturbed sea surface temperature experiments. *J. Geophys. Res.*, **102**, 19 383–19 402, doi:10.1029/97JD00206.

Donner, L. J., and H.-L. Kuo, 1984: Radiative forcing of stationary planetary waves. *J. Atmos. Sci.*, **41**, 2849–2868, doi:10.1175/1520-0469(1984)041<2849:RFOSPW>2.0.CO;2.

Feldl, N., and G. H. Roe, 2013: The nonlinear and nonlocal nature of climate feedbacks. *J. Climate*, **26**, 8289–8304, doi:10.1175/JCLI-D-12-00631.1.

Frierson, D. M. W., and Y.-T. Hwang, 2012: Extratropical influence on ITCZ shifts in slab ocean simulations of global warming. *J. Climate*, **25**, 720–733, doi:10.1175/JCLI-D-11-00116.1.

—, I. M. Held, and P. Zurita-Gotor, 2006: A gray-radiation aqua-planet moist GCM. Part I: Static stability and eddy scale. *J. Atmos. Sci.*, **63**, 2548–2566, doi:10.1175/JAS3753.1.

—, J. Lu, and G. Chen, 2007: Width of the Hadley cell in simple and comprehensive general circulation models. *Geophys. Res. Lett.*, **34**, L18804, doi:10.1029/2007GL031115.

Gastineau, G., H. A. Le Treut, and L. Li, 2008: Hadley circulation changes under global warming conditions indicated by coupled climate models. *Tellus*, **60A**, 863–884, doi:10.1111/j.1600-0870.2008.00344.x.

GFDD Global Atmospheric Model Development Team, 2004: The new GFDD global atmosphere and land model AM2-LM2: Evaluation with prescribed SST simulations. *J. Climate*, **17**, 4641–4673, doi:10.1175/JCLI-3223.1.

Hall, A., and S. Manabe, 1999: The role of water vapor feedback in unperturbed climate variability and global warming. *J. Climate*, **12**, 2327–2346, doi:10.1175/1520-0442(1999)012<2327:TROWVF>2.0.CO;2.

Hartmann, D. L., 1994: *Global Physical Climatology*. Academic Press, 411 pp.

—, and K. Larson, 2002: An important constraint on tropical cloud–climate feedback. *Geophys. Res. Lett.*, **29**, 1951, doi:10.1029/2002GL015835.

Harvey, B. J., L. C. Shaffrey, and T. J. Woollings, 2014: Equator-to-pole temperature differences and the extra-tropical storm track responses of the CMIP5 climate models. *Climate Dyn.*, **43**, 1171–1182, doi:10.1007/s00382-013-1883-9.

Held, I. M., 1993: Large-scale dynamics and global warming. *Bull. Amer. Meteor. Soc.*, **74**, 228–241, doi:10.1175/1520-0477(1993)074<0228:LSDAGW>2.0.CO;2.

—, and B. J. Soden, 2006: Robust responses of the hydrological cycle to global warming. *J. Climate*, **19**, 5686–5699, doi:10.1175/JCLI3990.1.

Hwang, Y.-T., and D. M. W. Frierson, 2010: Increasing atmospheric poleward energy transport with global warming. *Geophys. Res. Lett.*, **37**, L24807, doi:10.1029/2010GL045440.

—, —, and J. E. Kay, 2011: Coupling between Arctic feedbacks and changes in poleward energy transport. *Geophys. Res. Lett.*, **38**, L17704, doi:10.1029/2011GL048546.

Kidston, J., and E. P. Gerber, 2010: Intermodel variability of the poleward shift of the austral jet stream in the CMIP3 integrations linked to biases in 20th century climatology. *Geophys. Res. Lett.*, **37**, L09708, doi:10.1029/2010GL042873.

Knutson, T. R., and S. Manabe, 1995: Time-mean response over the tropical Pacific to increased CO₂ in a coupled ocean–atmosphere model. *J. Climate*, **8**, 2181–2199, doi:10.1175/1520-0442(1995)008<2181:TMROTT>2.0.CO;2.

Kushner, P. J., I. M. Held, and T. L. Delworth, 2001: Southern Hemisphere atmospheric circulation response to global warming. *J. Climate*, **14**, 2238–2249, doi:10.1175/1520-0442(2001)014<0001:SHACRT>2.0.CO;2.

Langen, P. L., R. G. Graversen, and T. Mauritsen, 2012: Separation of contributions from radiative feedbacks to polar amplification on an aquaplanet. *J. Climate*, **25**, 3010–3024, doi:10.1175/JCLI-D-11-00246.1.

Li, Y., D. W. J. Thompson, and S. Bony, 2015: The influence of atmospheric cloud radiative effects on the large-scale atmospheric circulation. *J. Climate*, **28**, 7263–7278, doi:10.1175/JCLI-D-14-00825.1.

Lorenz, D. J., 2014: Understanding midlatitude jet variability and change using Rossby wave chromatography: Poleward-shifted jets in response to external forcing. *J. Atmos. Sci.*, **71**, 2370–2389, doi:10.1175/JAS-D-13-0200.1.

—, and E. T. DeWeaver, 2007: Tropopause height and zonal wind response to global warming in the IPCC scenario integrations. *J. Geophys. Res.*, **112**, D10119, doi:10.1029/2006JD008087.

Lu, J., G. A. Vecchi, and T. Reichler, 2007: Expansion of the Hadley cell under global warming. *Geophys. Res. Lett.*, **34**, L06805, doi:10.1029/2006GL028443.

—, G. Chen, and D. M. W. Frierson, 2010: The position of the midlatitude storm track and eddy-driven westerlies in aquaplanet AGCMs. *J. Atmos. Sci.*, **67**, 3984–4000, doi:10.1175/2010JAS3477.1.

Mauritsen, T., R. G. Graversen, D. Klocke, P. L. Langen, B. Stevens, and L. Tomassini, 2013: Climate feedback efficiency and synergy. *Climate Dyn.*, **41**, 2539–2554, doi:10.1007/s00382-013-1808-7.

McCoy, D. T., D. L. Hartmann, and D. P. Grosvenor, 2014a: Observed Southern Ocean cloud properties and shortwave reflection. Part I: Calculation of SW flux from observed cloud properties. *J. Climate*, **27**, 8836–8857, doi:10.1175/JCLI-D-14-00287.1.

—, —, and —, 2014b: Observed Southern Ocean cloud properties and shortwave reflection. Part II: Phase changes and low cloud feedback. *J. Climate*, **27**, 8858–8868, doi:10.1175/JCLI-D-14-00288.1.

Merlis, T. M., 2014: Interacting components of the top-of-atmosphere energy balance affect changes in regional surface temperature. *Geophys. Res. Lett.*, **41**, 7291–7297, doi:10.1002/2014GL061700.

Pithan, F., and T. Mauritsen, 2014: Arctic amplification dominated by temperature feedbacks in contemporary climate models. *Nat. Geosci.*, **7**, 181–184, doi:10.1038/ngeo2071.

Roe, G. H., N. Feldl, K. C. Armour, Y.-T. Hwang, and D. M. W. Frierson, 2015: The remote impacts of climate feedbacks on regional climate predictability. *Nat. Geosci.*, **8**, 135–139, doi:10.1038/ngeo2346.

Schneider, E. K., B. P. Kirtman, and R. S. Lindzen, 1999: Tropospheric water vapor and climate sensitivity. *J. Atmos. Sci.*, **56**, 1649–1658, doi:10.1175/1520-0469(1999)056<1649:TWVAC>2.0.CO;2.

Senior, C. A., and J. F. B. Mitchell, 1993: Carbon dioxide and climate: The impact of cloud parameterization. *J. Climate*, **6**, 393–418, doi:10.1175/1520-0442(1993)006<0393:CDACTI>2.0.CO;2.

Sherwood, S. C., S. Bony, O. Boucher, C. Bretherton, P. M. Forster, J. M. Gregory, and B. Stevens, 2015: Adjustments in the forcing–feedback framework for understanding climate change. *Bull. Amer. Meteor. Soc.*, **96**, 217–228, doi:10.1175/BAMS-D-13-00167.1.

Simpson, I. R., T. A. Shaw, and R. Seager, 2014: A diagnosis of the seasonally and longitudinally varying midlatitude circulation response to global warming. *J. Atmos. Sci.*, **71**, 2489–2515, doi:10.1175/JAS-D-13-0325.1.

Slingo, A., and J. M. Slingo, 1988: The response of a general circulation model to cloud longwave radiative forcing. I: Introduction and initial experiments. *Quart. J. Roy. Meteor. Soc.*, **114**, 1027–1062, doi:10.1002/qj.49711448209.

Soden, B. J., I. M. Held, R. Colman, K. M. Shell, J. T. Kiehl, and C. A. Shields, 2008: Quantifying climate feedbacks using radiative kernels. *J. Climate*, **21**, 3504–3520, doi:10.1175/2007JCLI2110.1.

Tselioudis, G., W. B. Rossow, and D. Rind, 1992: Global patterns of cloud optical thickness variation with temperature. *J. Climate*, **5**, 1484–1495, doi:10.1175/1520-0442(1992)005<1484:GPOCOT>2.0.CO;2.

Tsushima, Y., and Coauthors, 2006: Importance of the mixed-phase cloud distribution in the control climate for assessing the response of clouds to carbon dioxide increase: a multi-model study. *Climate Dyn.*, **27**, 113–126, doi:10.1007/s00382-006-0127-7.

Vallis, G. K., P. Zurita-Gotor, C. Cairns, and J. Kidston, 2014: Response of the large-scale structure of the atmosphere to global warming. *Quart. J. Roy. Meteor. Soc.*, **141**, 1479–1501, doi:10.1002/qj.2456.

Vecchi, G. A., and B. J. Soden, 2007: Global warming and the weakening of the tropical circulation. *J. Climate*, **20**, 4316–4340, doi:10.1175/JCLI4258.1.

Vial, J., J.-L. Dufresne, and S. Bony, 2013: On the interpretation of inter-model spread in CMIP5 climate sensitivity estimates. *Climate Dyn.*, **41**, 3339–3362, doi:10.1007/s00382-013-1725-9.

Voigt, A., and T. A. Shaw, 2015: Circulation response to warming shaped by radiative changes of clouds and water vapour. *Nat. Geosci.*, **8**, 102–106, doi:10.1038/ngeo2345.

Wetherald, R. T., and S. Manabe, 1980: Cloud cover and climate sensitivity. *J. Atmos. Sci.*, **37**, 1485–1510, doi:10.1175/1520-0469(1980)037<1485:CCACS>2.0.CO;2.

—, and —, 1988: Cloud feedback processes in a general circulation model. *J. Atmos. Sci.*, **45**, 1397–1416, doi:[10.1175/1520-0469\(1988\)045<1397:CFPIAG>2.0.CO;2](https://doi.org/10.1175/1520-0469(1988)045<1397:CFPIAG>2.0.CO;2).

Yin, J. H., 2005: A consistent poleward shift of the storm tracks in simulations of 21st century climate. *Geophys. Res. Lett.*, **32**, L18701, doi:[10.1029/2005GL023684](https://doi.org/10.1029/2005GL023684).

Zelinka, M. D., and D. L. Hartmann, 2010: Why is longwave cloud feedback positive? *J. Geophys. Res.*, **115**, D16117, doi:[10.1029/2010JD013817](https://doi.org/10.1029/2010JD013817).

—, and —, 2012: Climate feedbacks and their implications for poleward energy flux changes in a warming climate. *J. Climate*, **25**, 608–624, doi:[10.1175/JCLI-D-11-00096.1](https://doi.org/10.1175/JCLI-D-11-00096.1).

—, S. A. Klein, and D. L. Hartmann, 2012: Computing and partitioning cloud feedbacks using cloud property histograms. Part II: Attribution to changes in cloud amount, altitude, and optical depth. *J. Climate*, **25**, 3736–3754, doi:[10.1175/JCLI-D-11-00249.1](https://doi.org/10.1175/JCLI-D-11-00249.1).